Prognostics in Highly Accelerated Limit Testing Using Deep Learning Data Analysis

Tadahiro Shibutani[1], Yuki Terauchi[2], and Yosuke Kikuchi[3]

[1]*Institute of Multidisciplinary Sciences, Yokohama National University, 79-5 Tokiwadai, Yokohama, 240-8501 Japan*
shibu@ynu.ac.jp

[2,3] *Department of Artificial environment engineering, Yokohama National University, 79-5 Tokiwadai, Yokohama, 240-8501 Japan*

ABSTRACT

In this study, an anomaly detection analysis of electronic components was conducted using deep learning algorithms on time-series data of voltage monitored during highly accelerated limit testing (HALT) on inverters used in automobiles and other vehicles. We demonstrated that the anomaly detection technology of time-series data using deep learning could detect equipment anomalies/failures to achieve effective data representation, improving the reliability assurance technology with HALT.

1. INTRODUCTION

A highly accelerated limit test (HALT) is a qualitative accelerated test to identify failure modes of products by applying external/internal stresses such as heating, cooling, vibration, and voltage ((International Electronics Commission, 2013). The operating or destructive limits are assessed to design the margin of products. The identified failure modes are treated as risks of products. The corrective actions are considered to improve products.

HALT has been used to detect faults in electrical products. IPC 9592B, which provides the requirements for power conversion devices, uses HALT as a design and qualification method. Dynabook Inc. emphasizes the quality of their products using HALT.

Though the main purpose of HALT is the identification of failure modes for products, it is not easy to identify failure modes of products during HALT. Chen et al. (2014) reported the application of HALT to improve DC/DC converter. They assessed three samples of DC/DC converter, and the functional degradation of the converter was found at a low-temperature limit. The sample resumed normal operation after the test. They tried to identify the failure mode of the converter, but the failure mode of the converter was not reported.

A typical method to identify failure modes of products is failure mode and effect analysis (FMEA). This method provides potential failure modes for each system component, and potential failure modes for each component are extracted based on the physics of failure. Hofmeister et al. (2010) proposed a diagnostics and prognostics tool for field programmable gate array (FPGA) devices and used HALT to confirm the validity of the tool. The four FPGA boards were assessed to identify failures due to thermal cycling and vibration stresses. Following the completion of HALT, the cross-section analysis confirmed that the fractures occurred at the solder ball joints of the FPGA. Sakamoto et al. (2018) assessed a small amplifier circuit board with FMEA and HALT. The FMEA was able to identify failure modes related to components. However, some failure modes observed in HALT resulted from the interaction between degraded components. FMEA often does not consider failure modes due to interactions between components.

Another approach is the data-driven approach. Anomaly behaviors of products are detected using data analysis techniques such as multivariate statics and/or machine learning. HALT requires functional testing to detect anomaly behaviors. The input/output variables are monitored to check the functional behaviors of products. Moreover, the detected anomaly behaviors are complex and difficult to understand. As HALT uses multiple stresses, such as thermal, mechanical, and electrical stresses, anomaly behaviors depend on interactions between multiple stresses. Therefore, the monitoring data are affected by several components due to the complexity of products.

The machine learning approach is an effective method for anomaly detection of functional tests with HALT. There are several algorithms proposed for the anomaly detection of data (Chandora, Banerjee, & Kumar, 2009). The nearest neighbor method is an unsupervised data driven approach for anomaly

detection. The anomaly scores are measured by the distance in the space of variables (Ramaswamy, Rastogi, & Shim, 2000). A fast outlier detection algorithm is also proposed (Angiulli & Pizzuti, 2002). However, the scores provide no information on failure modes. A support vector machine is a supervised approach to classification. Moreover, various linear and non-linear approaches have been proposed. Failure modes can be classified into supervised classes (Cho, Jo, Kim Park, & Park, 2020). Basudhar and Missoum (2013) proposed probabilistic support vector machines to estimate failure probability with Monte Carlo samples. However, identified failure modes are limited to supervised learning.

Deep learning is a state-of-the-art technique that is currently being researched for use in a wide range of fields, including image recognition, speech recognition, medicine, finance, security, and the military (Khan 2017). It can also be used to ensure the reliability of equipment in the engineering field. However, the amount of literature in the engineering field is small compared to other fields, and it is difficult to say that research activities are flourishing. In addition, most of the research papers are published from China, and even from a global perspective, there is a large regional bias and it is difficult to say that research is being conducted actively on a global scale (Khan & Yairi, 2017; Shao, Jiang, Zhao, & Wang, 2017; Sun, Shao, Zhao, Yan, Zhang, & Chen, 2016; Reddy, Sarkar, Venugopalan, & Giering, 2016; Zhao, Wang, Yan, & Mao, 2016; Xiang, Qu, Luo, Pu, & Tang, 2021; Vos, Peng, Jenkins, Shajriar, Borghesani, & Wang, 2022; Ye & Yu, 2021).

Shao et al. (2017) attempted to utilize deep autoencoders for fault diagnosis of rotating machinery, which is widely used in modern industry. In vibration analysis, which is currently the main method used, the vibration signals obtained are usually nonlinear and non-stationary, and useful failure characteristic information is often canceled out by heavy background noise, leading to inaccurate failure diagnosis. The deep autoencoder was used to extract feature information superior to failure diagnosis from the miscellaneous information obtained in the analysis, because of its simple structure and high efficiency.

Zhao et al. (2016) proposed an LSTM-based MHM algorithm for effectively monitoring equipment health. In the literature, raw sensory data was used to predict actual tool wear. The authors used LSTM as a prediction algorithm because it could capture long-term temporal dependencies. For comparison, single-layer LSTM, deep LSTM, and a conventional MHM method based on expert-generated features were considered. The analysis results showed that the LSTM model based on raw time-series data analysis outperformed the traditional expert top-down MHM method, and deep LSTM could learn more robust and abstract feature representations from the raw data. The deep LSTM predictions of tool wear progression were found to closely follow the actual wear condition of the tool as measured under a microscope.

Xiang et al. (2021) proposed an LSTM-based prediction model modified by the authors to accurately predict the remaining useful life (RUL) of aero engines. The authors attempted to develop an AI-based prediction model because of the lack of versatility, and traditional model-based approaches were difficult to apply to complex equipment such as aero engines. As the monitoring data obtained from the sensors around the aeroengine were time series, the authors considered LSTM to be the most suitable for RUL prediction. Accordingly, they designed a unit to determine the importance of the input data set and a multi-cellular unit with different data update modes based on the importance of the input data set. A unique improved model was constructed by incorporating a multi-cellular unit, and other units were designed to have different data update modes based on importance. To evaluate the proposed model, a demonstration of RUL prediction was conducted using open datasets of aero engines such as the widely used C-MAPSS. The demonstration results confirmed that the authors' proposed model outperformed traditional machine learning and deep learning-based RUL prediction.

Vos et al. (2022) attempted to develop an automated algorithm to identify any abnormal mechanical behavior captured by vibration measurements. They used as training data normal samples from a reduction gear endurance test and test flight data obtained from sensors installed at multiple locations on the helicopter, and designed a deep learning model combining LSTM and a one-class support vector machine (SVM) as an anomaly detection model. The model was designed as an anomaly detection model. In analyzing the data, by considering the physical mechanisms by which different failure modes (gearbox wear and bearing failure) affect the vibration signal, a two-stage model was designed: (1) an LSTM regression and 1-class SVM models to detect new deterministic features of the data set due to gearbox failure, and (2) an LSTM regression and 1-class SVM models to detect new random feature components generated in the data set by a bearing failure. The authors claimed that these improved task-specific LSTM models could detect abnormal machine failures from continuous time-series monitoring data with high accuracy by failure mode. However, they concluded that including LSTM did not improve the detection accuracy for continuous data sets, such as those consisting of multiple sensor data from different test flights of a helicopter. They also suggested that using a simple one-class SVM for outlier detection was more reasonable.

This study presents a method to identify failure modes of the inverter circuit at HALT with a machine-learning approach. The graphical model-based approaches were used to identify the failure modes. The neighborhood graph approach was employed to identify components related to failure modes. Gaussian graphical models were also used to investigate the interaction between components. Deep learning approaches were also adapted for anomaly detection of the inverter circuit due to HALT stresses.

2. EXPERIMENTAL PROCEDURE

2.1. Unit under Test

The unit under test in this study was a commercial inverter circuit board kit for learning (CQ Publishing). The functional block chart of the unit under test is shown in Figure 1. The unit consisted of a drive circuit board and a control circuit board. The three-phase motor was driven by supply voltage, and its speed was controlled by a 32-bit single-chip microcontroller (Renesas Electronics V850ES/FG3). A DC-to-DC converter (Cosel SUS62412) lowered the supply voltage to 12 V for the control circuit board. The microcontroller provided signals of PWM to the motor via gate driver IC and MOSFET (Infineon IRFZ48VPBF) based on the throttle of variable resistor. The Hall sensor attached to the motor sensed the rotating speed of three phase motor and fed it back to the microcontroller.

2.2. Highly Accelerated Limit Testing

The highly accelerated limit test (HALT) was conducted to identify the failure modes. HALT uses vibration and heat as stressors to identify failure modes as many products have failed due to vibration and/or temperature effects. HALT stressed the unit under test by applying cold, heat, rapid temperature change, and vibration.

The low-temperature stress step was started at 20 °C. The temperature decrease in the chamber was set to 10 °C every 10 minutes. The step was terminated when a malfunction of the unit appeared, and the temperature at the end of the step was defined as the lower operating limit (LOL). The high-temperature stress step was started at 30 °C. The temperature rise in the chamber was set to 10 °C every 10 minutes.

The rapid temperature change step is a stress step for specifying a failure mode of a product due to a rapid temperature change. The starting temperature was set between 20 [°C] and 30 [°C], and changed between the low-temperature and high-temperature sides. The temperature on the low-temperature side was the operation limit +10 [°C], confirmed by the low-temperature step stress test, and the temperature on the high-temperature side was the operation limit -10 [°C], confirmed by the high-temperature step stress test. The temperature was maintained constant for at least 5 minutes after the product temperature reached the set temperature. In addition, the temperature was changed at the maximum change rate given by the HALT tester. The testing was continued until a product failure was identified or a minimum of 5 temperature cycles were completed.

The vibration step stress test is a test for specifying a failure mode associated with vibration, including mechanical fatigue. Vibration is applied to the HALT tester's shaking table by random vibration of a total of six axes in translation and rotation directions with respect to two horizontal axes and one vertical axis. This vibration comprised a frequency component of 10 Hz to 5000 Hz. The test was started with an acceleration of 5 G_{rms}] and then increased the acceleration by 5 G_{rms}. The acceleration was kept constant for a minimum of 10 minutes at each acceleration. For 30 G_{rms} or more, it was recommended that after holding at each acceleration, reduce the acceleration to 5 G_{rms} and check whether the function was normal. The temperature during the test was maintained constant, considering the effect of self-heating of the product. The increase and hold of the acceleration will continue until the product failure is identified or the maximum acceleration given by the HALT tester, and if possible, the test will be continued until the failure limit can be confirmed.

The composite step stress test is a test for specifying a failure mode associated with a combined stress of vibration and rapid temperature change. The temperature change was obtained by a sudden temperature change cycle test method. The amount of increase in the vibration acceleration in each step was “the value obtained by dividing the value of the fracture limit confirmed in the vibration step stress test by 5”. At each acceleration, it was held for one cycle of the temperature cycle. The test was continued until a product failure was identified or this temperature cycle was performed for a minimum of 5 cycles.

Table 1. Monitoring data.

Measurement point	Monitoring parameter
1	Throttle voltage
2	Throttle supply voltage
3	Hall sensor output voltage (U phase)
4	Hall sensor output voltage (V phase)
5	Hall sensor output voltage (W phase)
6	Hall sensor supply voltage
7	Motor supply voltage (U phase)
8	Motor supply voltage (V phase)
9	Motor supply voltage (W phase)

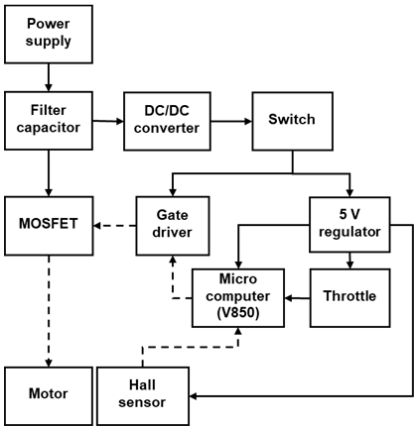

Figure 1. Functional block chart of the unit under test. The dashed arrows represent three-phase signal lines.

2.3. Experimental setup

The HALT chamber used was a commercial Qualmark Typhoon 2.5 chamber. The temperature range was -100–200 °C and the chamber had a vibrating table with 762 mm square. The inverter circuit board was assessed in the chamber. An aluminum plate (A5052P) jig was used to attach the substrate to the vibrating table. The motor body, Hall sensor, and throttle were installed outside the chamber, and the power supply voltage and signal voltage were measured while rotating the motor. Parameters monitored during HALT are listed in Table 1. LabVIEW of National Instruments was used for data acquisition. The sampling rate of parameters in Table 1 was 1,000 Sa/s. The temperature was measured by connecting a T-type thermocouple to Typhoon 2.5, and the sampling rate was 1 Sa/s. We used polyimide tape with excellent insulation and heat resistance when attaching the thermocouple to the inverter.

3. DATA ANALYSIS

We collected data from nine measurement points, as shown in Table 1. Data for each stress step were analyzed using machine learning. We employed a neighborhood graph approach and a Gaussian graphical model to identify the failure mechanism. The neighborhood graph approach was used to identify components related to observed anomaly behaviors. The Gaussian graphical model was used to characterize the interaction between components to anomaly behaviors.

3.1. Neighborhood graph approach

Ide (2009) proposed a neighborhood preservation principle (NPP) for anomaly analysis. NPP assumed that the neighborhood graph kept its structure under normal state. In other words, an anomaly of a system could be detected from a change in the neighborhood graph. The node exhibiting anomalous behavior could be identified by calculating the anomaly score of each node.

A training data set $\mathcal{D}_{\mathrm{tr}}$ and a test data set $\mathcal{D}$ were prepared to calculate the anomaly scores.

When N time series measurement data were obtained, the neighbor graph was constructed based on $N \times N$ dissimilarity matrix D. The element of D, $d_{i,j}$ is expressed as follows:

$$d_{i,j} = -log\left|\frac{c_{i,j}}{\sqrt{c_{i,i}c_{j,j}}}\right| \tag{1}$$

Here, $c_{i,j}$ is the covariance of time series data i and j. The neighbor graph was constructed based on D. The k-nearest neighbor graph for i-th node was a graph in which the i-th node was connected from the nearest neighbor to the k-th neighbor.

We used the probability $p(j|i)$ of the nearest neighbor pair of nodes j and i to express the change in the k-nearest neighbor graph quantitatively. $p(j|i)$ can be expressed as follows:

$$p(j|i) = \frac{1}{1+\sum_{l\in N_i} e^{-d_{i,l}}} e^{-d_{i,l}} \tag{2}$$

N_i is a set of k nearest neighbors, including the first nearest neighbor to the k-th nearest neighbor, for a node i. $p(j|i)$ takes zero when j is neither i nor N_i.

Anomaly score for node i could be calculated from the probabilities of the nearest neighbor pairs. Anomaly score of the node i is defined as follows:

$$E = max\left\{\left|\sum_{j\in N_i}\left(p(j|i) - \bar{p}(j|i)\right)\right|, \left|\sum_{j\in N_i}\left(p(j|i) - \bar{p}(j|i)\right)\right|\right\} \tag{3}$$

where $\bar{p}(j|i)$ is the probability of nearest neighbor pairs for the training data set, and $\bar{N}_i$ is a set of k nearest neighbors constructed by the training data set.

The training data were taken within 10 s after the beginning.

3.2. Deep learning algorithms

There are two types of learning methods in machine learning, including deep learning: (1) supervised learning, in which correct labels are prepared during learning and compared with AI output values, and (2) unsupervised learning, in which learning is performed using only normal data and the degree to which the input data deviates from normal is output as an anomaly. As it is difficult to label the time series data as normal/abnormal, using unsupervised learning in this analysis is appropriate. In this study, two unsupervised deep learning algorithms, called "Autoencoder" and " Long Short-Term Memory (LSTM)," are employed for comparison.

The auto-encoder model consists of two assumptions: an "encoder" that compresses the input data for low-dimensional data representation and a "decoder" that restores the original input data from the compressed data. Data compression in the encoder means that excess data is removed from the input data, and only data that is considered important for data representation is left. The data left by the encoder is called "features." Therefore, the essence of auto-encoders is a strategy for obtaining a function that calculates features from input data.

In this study, we employed the Deep Auto Encoder (DAE), which is a derivative model of the auto-encoder. The number of layers in the encoder and decoder portions was assumed to be equal and symmetric. According to the universality theorem, a neural network could approximate any function if it has at least one intermediate layer and a sufficiently large number of neurons. This would theoretically increase the expressive power and enable the representation of complex data such as large time-series data. In a previous study, a comparison of anomaly detection in time-series data by a general autoencoder and another derived model called deep auto encoder (DAE) and sparse auto-encoder was conducted, and it was confirmed that the deep auto-encoder has the highest data expressive power compared to the other two models, such as responding to more detailed anomalies. The DAE model responded to more detailed anomalies. Therefore, DAE was adopted as one of the analysis algorithms in this study.

As an effective model for anomaly detection in time series data, this study also employed an algorithm called LSTM, which is one of the most popular variations derived from the recurrent neural network (RNN), which was invented to handle sequential data. Moreover, it is one of the most popular models.

LSTM was invented by Sepp et al. (1997) as a solution to the "gradient loss/divergence problem" of RNNs. LSTM overcame the structural problems of RNNs by introducing memory cells with these features and achieved remarkable results in the field of time series data processing. In particular, LSTM was used to predict future data of time-series data, and it could be further applied to anomaly detection of time-series data. The model was constructed to predict the data at the time of detection. The LSTM model could output predictions with minimal error for normal data by learning to predict data using only normal data that did not contain anomalies. The LSTM model could detect anomalies in time series data using this property by judging that the input data contains anomalies when the prediction error is large. In this study, LSTM was employed as one of the anomaly analysis algorithms to analyze the results of the HALT test.

4. Results and Discussion

4.1. Summary of failure modes observed by HALT

Observed failure modes at HALT are summarized in Table 2. In the low-temperature step stress test, the motor stopped rotating when the set temperature was -50 °C. The test was terminated at this point. After the test was completed, the motor was recovered at room temperature. It means that destructive failure did not occur at the low-temperature stress step and the observation at -50 °C showed the occurrence of operating failure. The motor and power source were outside of the HALT chamber. The failure causes were dependent on the inverter circuit board. The drive power of the motor was supplied via the MOSFET with a filter capacitor. The operating temperature of MOSFET ranged from -55 to 175 °C. In this case, the power supply line to the motor worked.

The motor speed dropped at 130 °C in the high-temperature stress step test. After the stress step test, the motor was recovered at room temperature, and the operating failure occurred.

Based on low and high-temperature stress step tests, the temperature-changing test was conducted with five temperature cycles from -40 °C to 120 °C. No failure was confirmed after five cycles.

In the vibration stress step test, intermittent spike noises were observed at 35 G_{rms}, but the motor was operated normally. In this study, spike noises at 35 G_{rms} were defined as operating failure of UUT.

The combination stress step test was performed based on low/high-temperature stress step tests and vibration stress step tests. Five cycle temperature stresses were from -40 °C to 120 °C, and the acceleration of the shaking table was increased by 7 G_{rms} for each cycle. The motor stopped at 14 G_{rms} and -40 °C. The test was terminated and the motor was confirmed to be recovered at room temperature. The recovery of function indicates the operating failure occurred.

Table 2. Summary of HALT results.

Stresses	Result	Observation
Low temperature	-50 °C	Motor stopped
High Temperature	130 °C	Motor speed down
Rapid temperature change	N/A	No anomaly behavior
Vibration	35 Grms	Intermittent spike noises
Combined stresses	14 Grms (-40 °C)	Motor stopped

4.2. Identification of anomaly components

Figure 2 shows the anomaly scores of measuring points for the HALT stress steps. The degree of the neighborhood graph is set to 2 in the figure. The anomaly scores of throttle and Hall sensor supply voltages (measurement points 1, 2, and 6) were relatively high at low temperatures, rapid temperature change, and combined stress steps. The increase in anomaly score indicated that the topology of the neighborhood graph centered on the measurement point had changed. The throttle supply voltage (measurement point 2) had the highest value of anomaly score at the combined stress step where the motor stopped. The score at the low-temperature stress step was also high, and the motor stopped. The scores at the high-temperature stress step were less than 0.1, and a reduction in motor speed was observed. The score of the vibration stress step was more than 0.1 at measurement points 2 and 6. Intermittent spike noises were observed at the 35 G_{rms} of vibration stress. The highest value of anomaly score depended on the observed failure behaviors of the unit under test. The scores at Hall sensor output and motor supply voltage were less than 0.01. These values were not sensitive to the observed failure behaviors.

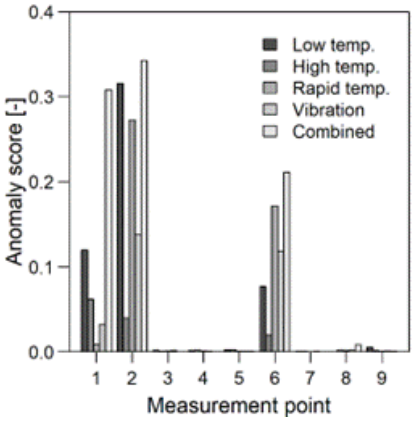

Figure 2. Anomaly scores of the unit under test by neighborhood graph approach (k=2).

4.3. Anomaly detection due to autoencoder

Abnormality detection using an auto-encoder showed a sharp increase in abnormality scores when the motors stopped rotating in the low-temperature step stress test and the combined stress step test. In the high-temperature step stress test, the increase in abnormality score was smaller than in the low-temperature stress test. This was because the abnormality at low temperatures was due to motor stoppage, whereas at high temperatures, it was a decrease in motor rotation speed. In other words, the auto-encoder abnormality score can be used as a measure of the degree of equipment abnormality. Moreover, in the vibration stress test, s-spike noise was observed at an average acceleration of 35 G_{rms} in the voltage measurements. However, the autoencoder showed an increase in abnormality only at some measurement points (1, 2, and 6).

Figure 3 shows the evolution in anomaly score of the motor supply voltage (U phase) by DAE. The results were obtained at the high-temperature stress step. In the experiment, the motor speed was observed to drop at 130 °C. However, the score indicated the anomaly alarm at 80 °C. This implied that the DAE worked as a precursor of anomaly detection for motors. As thermal reliability in electronics is a key issue, early detection of high-temperature stresses is expected to improve the reliability of electronics.

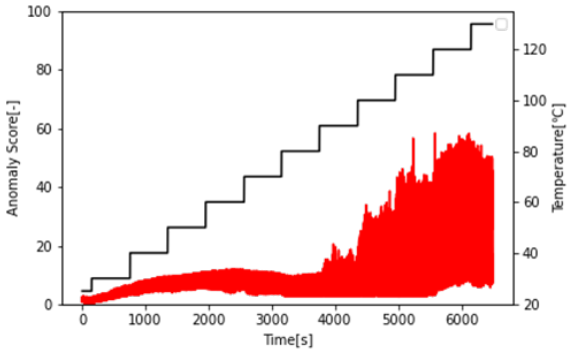

Figure 3. Anomaly score of motor supply voltage (Phase U) at high temperature stress step (deep autoencoder).

4.4. Anomaly detection due to LSTM

Figure 4 shows anomaly scores of the motor supply voltage (Phase U) obtained from LSTM. Comparing between two algorithms in Figures 3 and 4, the LSTM indicated the increase at -30 °C though the motor was observed to stop at -50 °C. However, the anomaly score of DAE showed a significant increase in the score at -50 °C. The autoencoder used the restoration error of the input data as the anomaly. As it detected anomalies only with the current value, it did not consider the behavior of past values or other time-series characteristics. Therefore, when a large anomaly occurred in the short term, the degree of abnormality was considered to have reacted drastically.

LSTM used prediction error, which compared the actual value with the output predicted from past values. In this method, the output at the time of a major failure was also affected by data from a small point in the past, leading to a gradual accumulation of anomaly severity and a response in anomaly severity at the point of stress level change rather than a sudden increase in the severity of anomaly.

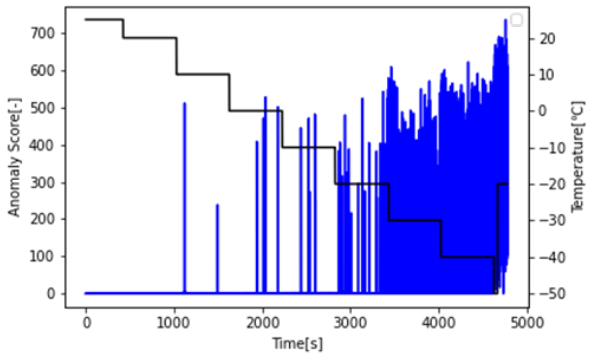

Figure 4. Anomaly score of motor supply voltage (Phase U) at low temperature stress step based on deep autoencoder and LSTM.

5. Conclusion

We conducted HALT to identify failure modes of an inverter circuit board for a three-phase motor. Failure modes were observed during the HALT. The three-phase motor was observed to stop at the low temperature stress and combination stress steps.

The data analysis implied that the anomaly behaviors observed were related to the throttle and Hall sensor power supply. The neighborhood graph approach successfully identified failure modes.

Deep learning approaches were used for anomaly detection of monitored data. DAE reacted to even small anomalies observed at the high-temperature stress step. These anomalies were not identified using the conventional machine learning approach, such as the k-th nearest neighbor method. LSTM was able to detect anomalies even earlier than DAE at the low-temperature stress step. Time-series monitoring data was suitable for LSTM because LSTM considers past time-series data.

References

Angiulli, F., Pizzuti, C. (2002) Fast Outlier Detection in High Dimensional Spaces. *Proceedings of European Conference on Principles of Data Mining and Knowledge Discovery*, pp. 15-26.

Basudhar, A. and Missoum, S. (2013) Reliability assessment using probabilistic support vector machines. *Int. J. Reliability and Safety*, Vol. 7, No. 2, pp. 156-173.

Chandora, V., Banerjee, A., Kumar, V. (2009). Anomaly detection: A survey. *ACM Computing Surveys*, Vol. 41, No. 3, pp. 1-58.

Chen, H., Yao, B., Xiao, Q. (2014). The study on application of HALT for DC/DC converter. *Proceedings of 2014 International Conference on Reliability, Maintainability and Safety (ICRMS)*, pp. 797-800.

Cho, K.-H., Jo, H.-C., Kim, E., Park, H.-A., Park, J.-H. (2020) Failure Diagnosis Method of Photovoltaic Generator Using Support Vector Machine. *Journal of Electrical Engineering & Technology*, Vol. 15, pp. 1669-1680.

Hochreiter, S. and Schmidhuber, J. (1997). Long Short Term Memory. *Neural Computation*, Vol. 9, No. 8, pp. 1735-1780.

Hofmeister, J. P., Vohnout, S., Mitchell, C., Heimes, F. O., Saha, S. (2010). HALT Evaluation of SJ BIST Technology for Electronic Prognostics. *Proceedings of International Automatic Testing Conference (IEEE AUTOTESTCON)*, September 13-16, Orlando, FL, USA. doi.org/10.1109/AUTEST.2010.5613585

Ide, T., Lozano, A., Abe, N., Liu, Y. (2009). Proximity-Based AnomalyDetection using Sparse Structure Learning, *Proceedings of the 2009 SIAM International Conference on Data Mining*, pp. 97-108. doi.org/10.1137/1.9781611972795.9

Infineon Technologies, IRFZ48VPbF Product Data Sheet, PD - 94992A, 2010.

International Electronics Comission (IEC) (2013). *Methods for product accelerated testing*, IEC 62506:2013.

Khan, S. and Yairi, T. (2017) A review on the application of deep learning in system health management. *Mechanical Systems and Signal Processing*, Vol. 107, pp. 241-265.

Ramaswamy, S., Rastogi, R. and Shim, K. (2000). Efficient algorithms for mining outliers from large data sets. *Proceedings of ACM Int. Conf. on Managment of Data (SIGMOD'00)*, pp. 427–438.

Reddy, K. K., Sarkar, S., Venugopalan, V., Giering, M. (2016). Anomaly detection and fault disambiguation in large flight data: A multi-modal Deep Auto-encoder approach. *Proceedings of Auunal Conference of the Prognostics and Health Management Society*. doi.org/10.36001/phmconf.2016.v8i1.2549

Sakamoto, J., Hirata, R., Shibutani, T. (2018). Potential failure mode identification of operational amplifier circuit board by using high accelerated limit test. *Microelectronics Reliability*, vol. 85, pp. 19-24.

Shao, H., Jiang, H., Zhao, H., Wang, F. (2017). A novel deep autoencoder feature learning method for rotating machinery fault dignosis. *Mechanical Systems and Signal Processing*, Vol. 95, pp. 187-204.

Sun, W., Shao, S., Zhao, R., Yan, R., Zhang, X., Chen, X. (2016). A sparse auto-encoder-based deep neural network approach for induction motor faults classification. *Measurement*, Vol. 89, pp. 171-178.

Vos, K., Peng, Z., Jenkins, C., Shajriar, M. R., Borghesani, P., Wang, W. (2022). Vibration-based anomaly detection using LSTM/SVM approaches. *Mechanical Systems and Signal Processing*, Vol. 169, 108752.

Xiang, S., Qu, Y., Luo, J., Pu, H., Tang, B. (2021) Multicellular LSTM-based deep learning model for aero-engine remaining useful life prediction. *Reliability Engineering and System Safety*, Vol. 216, 107927.

Ye, Z. and Yu, J. (2021). Health condition monitoring of machines based on long short term memory convolutional autoencoder. *Applied Soft Computing*, Vol. 17, 107379.

Zhao, R., Wang, J., Yan, R., Mao, K. (2016) Machine learning monitoring with LSTM network. *Proceedings of 10th International Conference on Sensing Technology*.